ACS APPLIED ELECTRONIC MATERIALS

pubs.acs.org/acsaelm

Article

Chemiresistive Device for the Detection of Nitroaromatic Explosives Based on Colloidal PbS Quantum Dots

Federica Mitri, Andrea De Iacovo,* Serena De Santis, Carlo Giansante, Giovanni Sotgiu, and Lorenzo Colace

Cite This: *ACS Appl. Electron. Mater.* 2021, 3, 3234−3239

Read Online

ACCESS | Metrics & More | Article Recommendations | Supporting Information

ABSTRACT: Semiconductor quantum dots have been recently employed as luminescent probes for the detection of hazardous nitroaromatic compounds. Despite the high sensitivity, such detection systems involve laboratory procedures and employ complex instrumentation. Here, we demonstrate the use of colloidal PbS quantum dots as the main component of a chemiresistor for the detection of nitroaromatic compounds. The proposed device is low-cost, reusable, and produces an electric signal that can be acquired with off-the-shelf electronic components. In this paper, we demonstrate the operation of the proposed device and we discuss its sensing mechanism. We also show the sensor's response to nitrobenzene in the 65 ppb−16 ppm range, estimating a theoretical detection limit of 2 ppb.

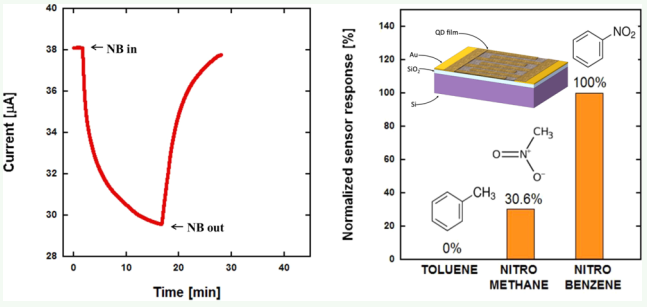

KEYWORDS: *quantum dots sensors, chemiresistive sensors, nitroaromatic explosives, room temperature sensing, trace detection*

INTRODUCTION

Detection of nitroaromatic compounds (NACs) vapor is essential for homeland security,[1] unrecovered land mines finding,[2] human health,[3] and environmental safety[4] since they are registered on the US Environmental Protection Agency's (EPA) list of priority pollutants for environmental remediation.[5] Apart from trained animals,[6] several detection methods are available including gas chromatography,[7] mass spectroscopy,[8] infrared spectroscopy,[9] surface-enhanced Raman scattering,[10] and ion mobility spectroscopy, which is a commonly used trace detection system in airports.[11] Although these methods allow for accurate measurements, they are time-consuming and expensive, requiring trained technical staff and dedicated equipment, and they are often confined to a laboratory environment. The current need to ensure fast and reliable detection of hazardous agents in numerous government agencies, airports, and public facilities requires miniaturized systems, characterized by high sensitivity, high portability, low power consumption, and low cost.[12] Gas sensors are a suitable technology to meet these needs, where the interaction of sensing materials with explosive molecules leads to observable outputs like a change in conductivity, color, or fluorescence.[13−15] In the last few years, many different approaches have been proposed for explosive sensing, employing a variety of materials.[16−19] Among all, sensors based on colloidal quantum dots (QD) have been widely investigated over the past few years as luminescent probes for the detection of a variety of analytes, including NACs. Colloidal QD offer several advantages for the realization of chemiresistors: (i) the colloidal stability of QD dispersions allows QD processing from the solution phase and deposition on several substrates; (ii) the high surface-to-volume ratio peculiar of the QD enlarges the possibilities of detecting analytes via QD surface chemistry modification; and (iii) the size-dependent electronic structure permits tuning of the QD energy levels that confers versatility in the use of different metal electrodes.

The majority of QD-based sensors are based either on photoinduced electron transfer (PET) or fluorescence resonance energy transfer (FRET) mechanisms. In the former case, the interaction between electron-rich surface-functionalized QD and electron-withdrawing NACs' nitro groups leads to the quenching of QD photoluminescence. In FRET-based sensors, a mixture of QD and a specific fluorophore is exposed to NAC vapors; the fluorophore can be chemically activated in the presence of NACs, thus inducing a shift of the fluorescence peak wavelength.[20,21] Several review papers on recent technologies for nitroaromatic explosive detection emphasized optical sensing using QD.[22−24] A multichannel QD array consisting of modified core−shell CdSe/ZnS QD was developed for the detection of five different explosives

Received: May 3, 2021
Accepted: June 21, 2021
Published: July 1, 2021

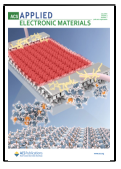

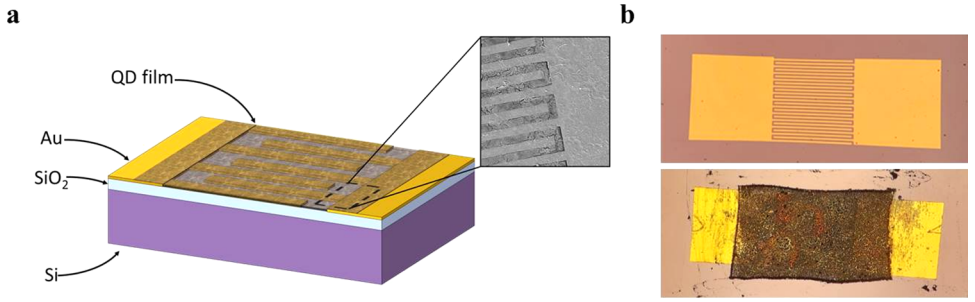

Figure 1. (a) Device schematic. (b) Optical microscopy images of the sensor before and after the deposition process. Metal fingers with a width of 5 μm and spacing are provided with 1 mm^2 bonding pads, with a sensing active area of 1 mm^2.

(DNT, TNT, tetryl, RDX, and PETN).[25] Each of the multicolor QD was functionalized with a different surface receptor via a facile ligation process. Komikawa et al. developed a chemical sensor for TNT using peptides conjugated to CdTe/CdS QD.[26] Moreover, a colorimetric sensor for the visual detection of TNT in the solution phase was also developed using a cysteamine-capped CdSe QD-decorated graphene−chitosan xerogel.[27]

Despite the successful demonstration of sensitive detection of NACs based on QD photoluminescence quenching, the proposed approaches still consist of lab-based procedures and do not produce actual sensors. A more promising approach toward the realization of compact and easy-to-use devices could be an NAC detector based on conductivity changes of functionalized QD. To this extent, QD's properties such as the large surface-to-volume ratio, surface reactivity even at room temperature, and the possibility to engineer their properties through surface chemistry can be effectively exploited.[28]

Sensors based on the change of conductivity are potentially advantageous with respect to those based on photoluminescence quenching since they can be easily implemented in low-power and low-cost electronics. In addition, their fabrication is suitable for integration with silicon technology.

Gas sensors based on PbS QD have already been demonstrated, but there are no examples to date of QD-based chemiresistors for NAC detection.[29−34] In this article, we report on a novel and high-performance chemiresistive sensor based on PbS QD for the detection of traces of nitroaromatic explosives at room temperature. The conductivity of an ethylenediamine (EDA)-functionalized QD film is analyzed, showing substantial modification upon NAC exposure, with nitrobenzene (NB) as a representative compound. We also discuss the detection mechanism of the devices, showing their selectivity to NACs with respect to nitro aliphatic compounds and aromatic compounds without electron-withdrawing groups.

EXPERIMENTAL DETAILS

The synthesis of colloidal PbS QD was performed in a three-neck flask connected to a standard Schlenk line under oxygen and water-free conditions;[35] detailed synthetic and purification procedures are given in the Supporting Information (SI). The synthetic procedure yielded colloidal PbS QD with a diameter of about 4.7 nm, and 0.5 mM toluene dispersions were used for device fabrication; transmission electron microscopy and optical absorption measurements were used to estimate QD size and concentration.[36] Prepatterned gold interdigitated electrodes (IDE) on a silicon chip were used as deposition substrates (see Figure 1a,b). Each substrate contained five couples of IDE. Devices were fabricated through layer-by-layer spin coating of PbS QD dispersions followed by in situ ligand exchange with ethylenediamine (EDA).[37] For each layer, the following steps were performed: (1) an 8 μL drop of the QD dispersion was deposited onto the substrate and spun at 3000 rpm for 30 s; (2) two 8 μL drops of 10% v/v ethylenediamine in acetonitrile were deposited on the QD, allowed to exchange pristine ligands for 60 s, and then spun at 3000 rpm for 30 s; and (3) the obtained film was rinsed with ethanol while spinning at 3000 rpm for 30 s to wash off unbound ligands and loosely deposited QDs. The above fabrication process was repeated up to 10 times to grow a QD film with a thickness of about 200 nm, as measured by surface profilometry (see the SI).

Figure 2 shows a typical Fourier transform infrared (FTIR) spectrum recorded from a finished sensor, compared with a reference

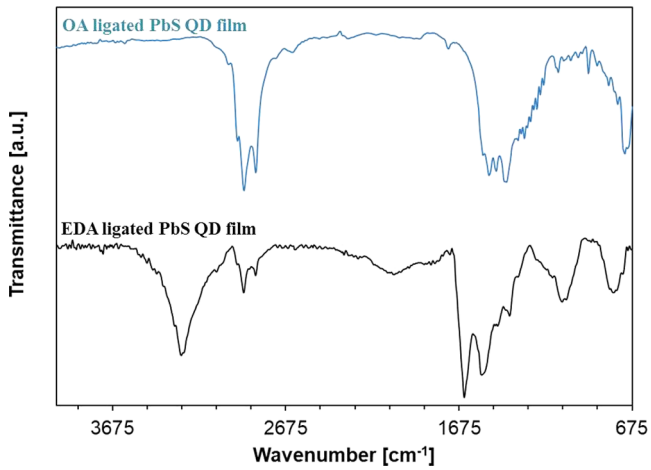

Figure 2. FTIR spectrum of the fabricated device.

device, in which the QD were not ligand-exchanged. The bands centered at 3310 and 1650 cm^{-1} were assigned to the N−H stretching vibration, confirming that EDA effectively attached to the surface of PbS QD.

Control devices were also realized by substituting EDA with tetrabutylammonium iodide (TBAI). In that case, ligand exchange was carried out by rinsing the device in a 10 mg/mL TBAI/MeOH solution for 60 s after every QD deposition step, followed by washing with isopropanol. A detailed fabrication process is reported elsewhere.[38]

The sensor response was assessed by employing NB as a representative NAC. To evaluate its performance, the sensor was placed in a custom-made chamber equipped with humidity and temperature sensors. A direct current (DC) voltage of 1 V was applied to the sensor, and the current was measured during target gas exposure and release. The sensor was operated at room temperature and 30% controlled humidity and it was tested for different NB concentrations ranging from 65 ppb to 16 ppm. In a typical experiment, the measurement chamber was flushed with ambient air until the sensor current became stable. Therefore, the NB gas was diluted with air through two mass flowmeters to reach the desired

https://doi.org/10.1021/acsaelm.1c00401
ACS Appl. Electron. Mater. 2021, 3, 3234−3239

concentration and was allowed to flow through the chamber. The gas flow was kept constant (800 mL/min) and the device's current was monitored continuously. When the device's current became constant again (typically after a few minutes), the chamber was purged with clean air to recover the sensor. A detailed description of the experimental setup and procedures as well as the calculation of NB concentration is available in the SI. Sensor performance was evaluated through the sensor response (S), expressed in percentage, and calculated according to eq 1, where I_a and I_g are the initial current and its value after exposure to a given vapor concentration of the target gas, respectively.

$$S = \frac{I_a - I_g}{I_a} \times 100 \quad (1)$$

The response time is defined as the time required to achieve 90% of the total current change upon exposure to the target gas. The recovery time is the time required to reach 10% of the total current change after purging the measurement chamber with clean air.

RESULTS AND DISCUSSION

Figure 3 shows a typical time response of the sensor current to 1.87 ppm NB vapor at room temperature.

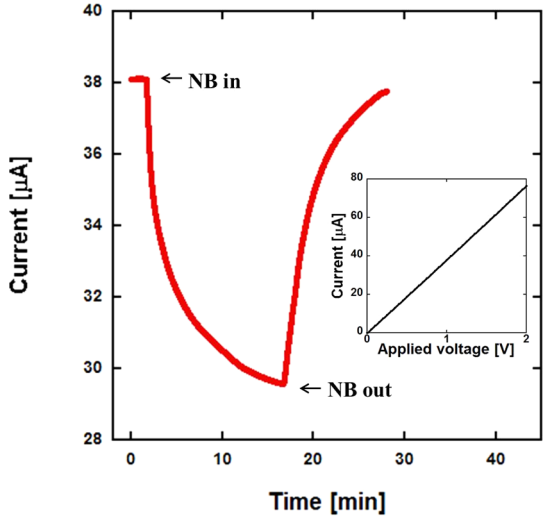

Figure 3. Real-time current change obtained with 1.87 ppm NB. The inset shows the $I-V$ curve upon nitrobenzene exposure.

The sensor current reached a steady state of about 38 μA in ambient air and when the NB gas entered the measurement chamber, the current rapidly decreased, reaching a minimum value of 29.5 μA. A full baseline recovery was obtained after gas release, thus implying a reversible adsorption/desorption characteristic for the NB vapor of the QD-based sensing film. The analyte exposure time was 15 min with a sensor response of 22.2%, whereas the response and recovery times were 9.6 and 8.7 min, respectively. The inset shows a typical current−voltage characteristic of the device upon NB exposure. The linear behavior confirmed the expected ohmic characteristic of the QD/metal contact in both ambient air and in the presence of NB. The typical measured current I_a at 1 V in air was about 38 μA with a corresponding resistance R_d of 26.3 kΩ. The sensor response of the PbS QD device with NB concentration varying from 65 to 655 ppb was also measured and is reported in Figure 4a. Specifically, six cycles of gas exposure and purge were successively recorded, corresponding to NB gas concentrations of 65, 98, 164, 327, 491, and 655 ppb. After every measurement, the devices showed excellent reversibility and negligible baseline drift. Table S1 reports the S value for all of the measured NB concentrations.

As expected, the sensor response increased with the NB concentration, exhibiting linear behavior at low concentrations and clear saturation above few ppm. The inset of Figure 4b shows a linear fit of the sensor $\Delta I = (I_a - I_g)$ versus NB concentration in the low-concentration range (from 65 to 655 ppb). Here, the theoretical detection limit of the device has been estimated. The slope of the linearized characteristic was 0.82 μA/ppm with a correlation coefficient of 0.97. A detection limit (DL) of 2 ppb was estimated for NB at room temperature, with a signal-to-noise ratio (SNR) of 3, according to the following equation[39]

$$\mathrm{DL} = 3\frac{i_n}{\Theta} \quad (2)$$

where i_n is the root-mean-squared (RMS) current noise and Θ is the slope of the current/NB concentration characteristic. The noise current was evaluated using the standard deviation over 500 data points acquired in a 3 min time span in the baseline of the response curve (see the SI for more details). According to eq 2, the maximum sensitivity is calculated as the

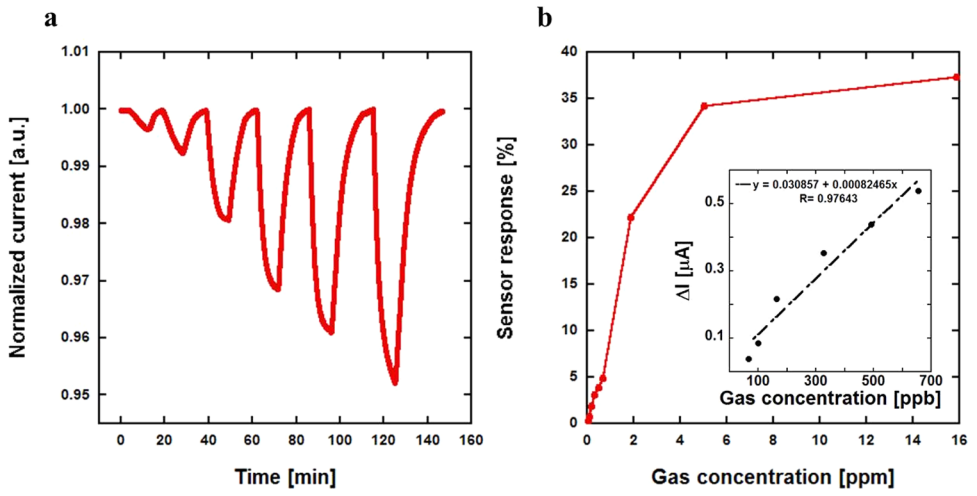

Figure 4. (a) Normalized current curves toward different concentrations of NB as a function of time. (b) Sensor $\Delta I = (I_a - I_g)$ to different NB concentrations. The inset shows the linear fitting in the 65−655 ppb range.

https://doi.org/10.1021/acsaelm.1c00401
ACS Appl. Electron. Mater. 2021, 3, 3234−3239

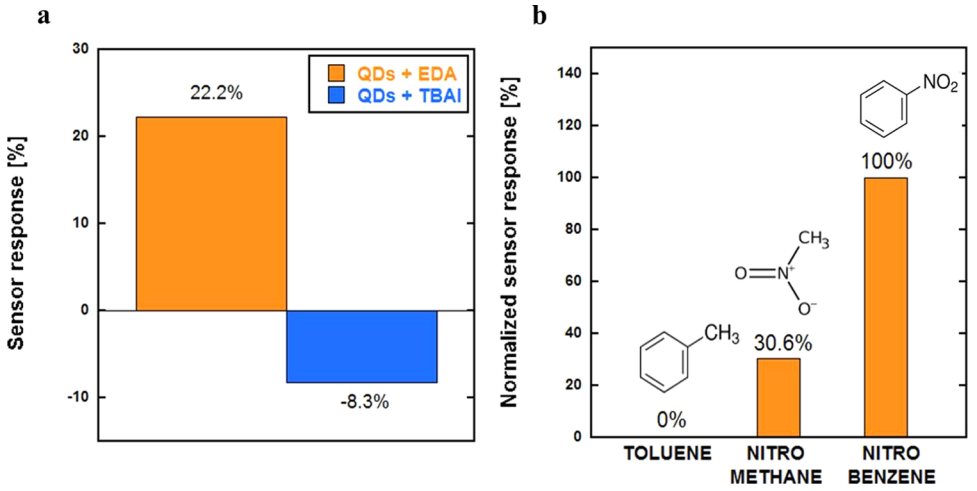

Figure 5. (a) Sensor responses of the EDA-capped sensor and the TBAI-treated sensor to 1.87 ppm NB. (b) Sensor response of the EDA-capped PbS QD sensor to toluene, nitromethane, and nitrobenzene at the same concentration of 5 ppm, normalized with respect to the sensor response value for NB.

concentration that produces a current signal 3 times larger (about 10 dB) than the noise current. This figure helps to estimate the potential sensitivity of the device at concentrations below the limit of the experimental setup. The sensor exhibited very large sensitivity in terms of both the lowest measured (65 ppb) and lowest estimated (2 ppb) NB concentrations. Such performance can be ascribed to a combination of both low noise and large sensor responses. While current noise is kept low thanks to the large device resistivity and a low noise electronic front end, the sensor response is related to the large PbS QD surface-to-volume ratio and to the employment of EDA as a surface ligand. In fact, the device's sensing mechanism is strictly related to EDA, which plays a fundamental role in NAC detection. The interactions at the QD surface between the electron-rich amine ligands and the electron-deficient aromatic ring may occur, eventually leading to the formation of adducts referable to Meisenheimer-like complexes. The resulting EDA-to-NB charge transfer could be responsible for the significant decrease of the QD film current signal. The same reaction mechanism has already been exploited in explosive detectors based on the quenching of QD photoluminescence.[22]

To support this hypothesis, the sensing performance of the EDA-capped PbS QD sensor was compared with the performance of the PbS QD sensor where a different ligand (TBAI) was employed. Figure 5a shows the results from both sensors exposed to 1.87 ppm NB at room temperature.

The TBAI-treated sensor showed a sensor response as low as 8.3% to 1.87 ppm NB, significantly lower than that observed for EDA-capped devices exposed to the same amount of NB. In addition, nitromethane and toluene were selected to investigate the effects of aromaticity and polarity of the chemical vapor on the conductivity of the sensor. Indeed, nitromethane has an electron-withdrawing group but is not aromatic, whereas toluene is aromatic but with an electron-donating group. Figure 5b shows the normalized sensor response toward these chemical vapors (5 ppm). As expected, the results highlighted a remarkably selective change in conductivity for NB over NM, while no response was observed upon exposure to toluene gas. This observation confirms the preferential electronic interaction between EDA and the electron-poor benzenic ring of NB.

CONCLUSIONS

In summary, this work demonstrates that the change in conductivity of an EDA-capped PbS QD sensor can be effectively used for the room temperature vapor detection of nitrobenzene. The sensor was fabricated through a simple, rapid, and low-cost method. The sensor showed high sensitivity to NB, as representative of the electron-deficient nitroaromatics, in addition to rapid response and full recovery after gas release. A sensor response of 0.34% has been measured to a NB concentration of as low as 65 ppb, and a detection limit of 2 ppb was estimated from the slope of the sensor response and noise measurements. The proposed sensor has the potential to be further optimized with the aim to be integrated into a portable, miniaturized, and inexpensive device for the detection of explosives in strategic and sensitive environments.

ASSOCIATED CONTENT

Supporting Information

The Supporting Information is available free of charge at https://pubs.acs.org/doi/10.1021/acsaelm.1c00401.

Synthesis of colloidal PbS QD; fabrication process of the ethylenediamine-capped PbS QD sensor; PbS QD film thickness; experimental setup and procedure; calculation of vapor concentration; and calculation of the detection limit (PDF)

AUTHOR INFORMATION

Corresponding Author

Andrea De Iacovo − *Department of Engineering and CNIT - Consorzio Nazionale Interuniversitario per le Telecomunicazioni, University Roma Tre, Rome 00146, Italy*; orcid.org/0000-0001-5006-5505; Email: andrea.deiacovo@uniroma3.it

Authors

Federica Mitri − *Department of Engineering, University Roma Tre, Rome 00146, Italy*

Serena De Santis − *Department of Engineering, University Roma Tre, Rome 00146, Italy*

Carlo Giansante − *CNR Nanotec, Istituto di Nanotecnologia, Lecce 73100, Italy;* orcid.org/0000-0003-4558-5367
Giovanni Sotgiu − *Department of Engineering, University Roma Tre, Rome 00146, Italy*
Lorenzo Colace − *Department of Engineering and CNIT - Consorzio Nazionale Interuniversitario per le Telecomunicazioni, University Roma Tre, Rome 00146, Italy*

Complete contact information is available at: https://pubs.acs.org/10.1021/acsaelm.1c00401

Author Contributions

A.D.I. and L.C. conceived the original idea and designed the device; F.M., A.D.I., and S.D.S. carried out the experiments; G.S. contributed to data analysis and discussion; and C.G. synthesized the QD dispersions. All authors contributed equally to the manuscript redaction and review.

Funding

C.G. thanks Progetto di ricerca MIUR PON 2014-2020, Energia per l'Ambiente TARANTO (Project no.: ARS01_00637).

Notes

The authors declare no competing financial interest.

■ ABBREVIATIONS

EDA, ethylenediamine; IDE, interdigitated electrodes; NACs, nitroaromatic compounds; NB, nitrobenzene; NM, nitromethane; OA, oleic acid; OM, optical microscopy; PbS, lead sulfide; QD, quantum dots; TBAI, tetrabutylammonium iodide

■ REFERENCES

(1) Caygill, J. S.; Davis, F.; Higson, S. P. J. Current Trends in Explosive Detection Techniques. *Talanta* **2012**, *88*, 14−29.
(2) Lefferts, M. J.; Castell, M. R. Vapour Sensing of Explosive Materials. *Anal. Methods* **2015**, *7*, 9005−9017.
(3) Chandra, S. A.; Nolan, M. W.; Malarkey, D. E. Chemical Carcinogenesis of the Gastrointestinal Tract in Rodents: An Overview with Emphasis on NTP Carcinogenesis Bioassays. *Toxicol. Pathol.* **2010**, *38*, 188−197.
(4) Lu, W.; Li, H.; Meng, Z.; Liang, X.; Xue, M.; Wang, Q.; Dong, X. Detection of Nitrobenzene Compounds in Surface Water by Ion Mobility Spectrometry Coupled with Molecularly Imprinted Polymers. *J. Hazard. Mater.* **2014**, *280*, 588−594.
(5) Keith, L. H.; Telliard, W. A. Priority Pollutants. I. A Perspective View. *Environ. Sci. Technol.* **1979**, *13*, 416−423.
(6) Furton, K. G.; Myers, L. J. The Scientific Foundation and Efficacy of the Use of Canines as Chemical Detectors for Explosives. *Talanta* **2001**, *54*, 487−500.
(7) Walsh, M. E. Determination of Nitroaromatic, Nitramine, and Nitrate Ester Explosives in Soil by Gas Chromatography and an Electron Capture Detector. *Talanta* **2001**, *54*, 427−438.
(8) Badjagbo, K.; Sauvé, S. Mass Spectrometry for Trace Analysis of Explosives in Water. *Crit. Rev. Anal. Chem.* **2012**, *42*, 257−271.
(9) Ewing, A. V.; Kazarian, S. G. Infrared Spectroscopy and Spectroscopic Imaging in Forensic Science. *Analyst* **2017**, *142*, 257−272.
(10) Botti, S.; Almaviva, S.; Cantarini, L.; Palucci, A.; Puiu, A.; Rufoloni, A. Trace Level Detection and Identification of Nitro-Based Explosives by Surface-Enhanced Raman Spectroscopy. *J. Raman Spectrosc.* **2013**, *44*, 463−468.
(11) Buryakov, I. A. Detection of Explosives by Ion Mobility Spectrometry. *J. Anal. Chem.* **2011**, *66*, 674−694.
(12) Gares, K. L.; Hufziger, K. T.; Bykov, S. V.; Asher, S. A. Review of Explosive Detection Methodologies and the Emergence of Standoff Deep UV Resonance Raman. *J. Raman Spectrosc.* **2016**, *47*, 124−141.
(13) Singh, S. Sensors-An Effective Approach for the Detection of Explosives. *J. Hazard. Mater.* **2007**, *144*, 15−28.
(14) Bielecki, Z.; Janucki, J.; Kawalec, A.; Mikołajczyk, J.; Pałka, N.; Pasternak, M.; Pustelny, T.; Stacewicz, T.; Wojtas, J. Sensors and systems for the detection of explosive devices − an overview. *Metrol. Meas. Syst.* **2012**, *XIX*, 3−28.
(15) Müller, G.; Hackner, A.; Beer, S.; Göbel, J. Solid-State Gas Sensors: Sensor System Challenges in the Civil Security Domain. *Materials* **2016**, *9*, No. 65.
(16) Yang, Z.; Dou, X.; Zhang, S.; Guo, L.; Zu, B.; Wu, Z.; Zeng, H. A High-Performance Nitro-Explosives Schottky Sensor Boosted by Interface Modulation. *Adv. Funct. Mater.* **2015**, *25*, 4039−4048.
(17) Qu, J.; Ge, Y.; Zu, B.; Li, Y.; Dou, X. Transition-Metal-Doped p-Type ZnO Nanoparticle-Based Sensory Array for Instant Discrimination of Explosive Vapors. *Small* **2016**, *12*, 1369−1377.
(18) Wu, Z. F.; Zhou, C. Y.; Zu, B. Y.; Li, Y. S.; Dou, X. C. Contactless and Rapid Discrimination of Improvised Explosives Realized by Mn2+ Doping Tailored ZnS Nanocrystals. *Adv. Funct. Mater.* **2016**, *26*, 4578−4586.
(19) Liu, Y.; Li, J.; Wang, G.; Zu, B.; Dou, X. One-Step Instantaneous Detection of Multiple Military and Improvised Explosives Facilitated by Colorimetric Reagent Design. *Anal. Chem.* **2020**, *92*, 13980−13988.
(20) Chou, K. F.; Dennis, A. M. Förster Resonance Energy Transfer between Quantum Dot Donors and Quantum Dot Acceptors. *Sensors* **2015**, *15*, 13288−13325.
(21) Wang, S.; Li, N.; Pan, W.; Tang, B. Advances in Functional Fluorescent and Luminescent Probes for Imaging Intracellular Small-Molecule Reactive Species. *TrAC, Trends Anal. Chem.* **2012**, *39*, 3−37.
(22) Akhgari, F.; Fattahi, H.; Oskoei, Y. M. *Recent Advances in Nanomaterial-Based Sensors for Detection of Trace Nitroaromatic Explosives*; Elsevier B.V., 2015; Vol. *221*.
(23) Ma, Y.; Wang, S.; Wang, L. Nanomaterials for Luminescence Detection of Nitroaromatic Explosives. *TrAC, Trends Anal. Chem.* **2015**, *65*, 13−21.
(24) To, K. C.; Ben-Jaber, S.; Parkin, I. P. Recent Developments in the Field of Explosive Trace Detection. *ACS Nano* **2020**, *14*, 10804−10833.
(25) Peveler, W. J.; Roldan, A.; Hollingsworth, N.; Porter, M. J.; Parkin, I. P. Multichannel Detection and Differentiation of Explosives with a Quantum Dot Array. *ACS Nano* **2016**, *10*, 1139−1146.
(26) Komikawa, T.; Tanaka, M.; Tamang, A.; Evans, S. D.; Critchley, K.; Okochi, M. Peptide-Functionalized Quantum Dots for Rapid Label-Free Sensing of 2,4,6-Trinitrotoluene. *Bioconjugate Chem.* **2020**, *31*, 1400−1407.
(27) Kumar, V.; Kumar, A.; Nath, P.; Satapathi, S. Fabrication of Cysteamine Capped-CdSe QDs Anchored Graphene Xerogel Nanosensor for Facile Onsite Visual Detection of TNT. *Nano-Struct. Nano-Objects* **2021**, *25*, No. 100643.
(28) Kagan, C. R.; Lifshitz, E.; Sargent, E. H.; Talapin, D. V. Building Devices from Colloidal Quantum Dots. *Science* **2016**, *353*, No. aac5523.
(29) Liu, H.; Li, M.; Voznyy, O.; Hu, L.; Fu, Q.; Zhou, D.; Xia, Z.; Sargent, E. H.; Tang, J. Physically Flexible, Rapid-Response Gas Sensor Based on Colloidal Quantum Dot Solids. *Adv. Mater.* **2014**, *26*, 2718−2724.
(30) Mitri, F.; De Iacovo, A.; De Luca, M.; Pecora, A.; Colace, L. Lead Sulphide Colloidal Quantum Dots for Room Temperature NO2 Gas Sensors. *Sci. Rep.* **2020**, *10*, No. 12556.
(31) Liu, H.; Li, M.; Shao, G.; Zhang, W.; Wang, W.; Song, H.; Cao, H.; Ma, W.; Tang, J. Enhancement of Hydrogen Sulfide Gas Sensing of PbS Colloidal Quantum Dots by Remote Doping through Ligand Exchange. *Sens. Actuators, B* **2015**, *212*, 434−439.
(32) Li, M.; Zhou, D.; Zhao, J.; Zheng, Z.; He, J.; Hu, L.; Xia, Z.; Tang, J.; Liu, H. Resistive Gas Sensors Based on Colloidal Quantum Dot (CQD) Solids for Hydrogen Sulfide Detection. *Sens. Actuators, B* **2015**, *217*, 198−201.

(33) Mosahebfard, A.; Dehdashti Jahromi, H.; Sheikhi, M. H. Highly Sensitive, Room Temperature Methane Gas Sensor Based on Lead Sulfide Colloidal Nanocrystals. *IEEE Sens. J.* **2016**, *16*, 4174−4179.
(34) Liu, Y.; Wang, L.; Wang, H.; Xiong, M.; Yang, T.; Zakharova, G. S. Highly Sensitive and Selective Ammonia Gas Sensors Based on PbS Quantum Dots/TiO2 Nanotube Arrays at Room Temperature. *Sens. Actuators, B* **2016**, *236*, 529−536.
(35) Giansante, C. Surface Chemistry Control of Colloidal Quantum Dot Band Gap. *J. Phys. Chem. C* **2018**, *122*, 18110−18116.
(36) Debellis, D.; Gigli, G.; Ten Brinck, S.; Infante, I.; Giansante, C. Quantum-Confined and Enhanced Optical Absorption of Colloidal PbS Quantum Dots at Wavelengths with Expected Bulk Behavior. *Nano Lett.* **2017**, *17*, 1248−1254.
(37) Kundu, B.; Pal, A. J. Ligand-Mediated Energy-Level Modification in PbS Quantum Dots as Probed by Density of States (DOS) Spectra. *J. Phys. Chem. C* **2018**, *122*, 11570−11576.
(38) Venettacci, C.; Martin-Garcia, B.; Prato, M.; Moreels, I.; De Iacovo, A. Increasing Responsivity and Air Stability of PbS Colloidal Quantum Dot Photoconductors with Iodine Surface Ligands. *Nanotechnology* **2019**, *30*, No. 405204.
(39) Dua, V.; Surwade, S. P.; Ammu, S.; Agnihotra, S. R.; Jain, S.; Roberts, K. E.; Park, S.; Ruoff, R. S.; Manohar, S. K. All-Organic Vapor Sensor Using Inkjet-Printed Reduced Graphene Oxide. *Angew. Chem., Int. Ed.* **2010**, *49*, 2154−2157.

https://doi.org/10.1021/acsaelm.1c00401
ACS Appl. Electron. Mater. 2021, 3, 3234−3239